

# Automatic Segmentation of Dental Root Canal and Merging with Crown Shape

Romain Deleat-Besson<sup>1</sup>, Celia Le<sup>1</sup>, Najla Al Turkestani<sup>1</sup>, Winston Zhang<sup>1</sup>, Maxime Dumont<sup>1</sup>, Serge Brosset<sup>1</sup>, Juan Carlos Prieto<sup>2</sup>, Lucia Cevdanes<sup>1</sup>, Jonas Bianchi<sup>1</sup>, Antonio Ruellas<sup>1</sup>, Marcela Gurgel<sup>1</sup>, Camila Massaro<sup>1</sup>, Aron Aliaga-Del Castillo<sup>1</sup>, Marcos Ioshida<sup>1</sup>, Marilia Yatabe<sup>1</sup>, Erika Benavides<sup>1</sup>, Hector Rios<sup>1</sup>, Fabiana Soki<sup>1</sup>, Gisele Neiva<sup>1</sup>, Juan Fernando Aristizabal<sup>3</sup>, Diego Rey<sup>4</sup>, Maria Antonia Alvarez<sup>4</sup>, Kayvan Najarian<sup>4</sup>, Jonathan Gryak<sup>4</sup>, Martin Styner<sup>2</sup>, Jean-Christophe Fillion-Robin<sup>5</sup>, Beatriz Paniagua<sup>5</sup>, Reza Soroushmehr<sup>4</sup>

**Abstract**— In this paper, machine learning approaches are proposed to support dental researchers and clinicians to study the shape and position of dental crowns and roots, by implementing a Patient Specific Classification and Prediction tool that includes RootCanalSeg and DentalModelSeg algorithms and then merges the output of these tools for intraoral scanning and volumetric dental imaging. RootCanalSeg combines image processing and machine learning approaches to automatically segment the root canals of the lower and upper jaws from large datasets, providing clinical information on tooth long axis for orthodontics, endodontics, prosthodontic and restorative dentistry procedures. DentalModelSeg includes segmenting the teeth from the crown shape to provide clinical information on each individual tooth. The merging algorithm then allows users to integrate dental models for quantitative assessments. Precision in dentistry has been mainly driven by dental crown surface characteristics, but information on tooth root morphology and position is important for successful root canal preparation, pulp regeneration, planning of orthodontic movement, restorative and implant dentistry. In this paper we propose a patient specific classification and prediction of dental root canal and crown shape analysis workflow that employs image processing and machine learning methods to analyze crown surfaces, obtained by intraoral scanners, and three-dimensional volumetric images of the jaws and teeth root canals, obtained by cone beam computed tomography (CBCT).

## INTRODUCTION

Comprehensive dentistry treatments aim to keep the integrity of soft tissues bones, and teeth. Machine learning techniques have been successfully used for automatically isolating anatomical structures of interest in dental crown and root imaging [1]. Risk factors of root resorption [2-4] as well as stress distribution of orthodontic and restorative procedures require assessments of root morphology and the long axis of the teeth [5-7]. Severe root resorption has been reported in 7% to 15% of the population, and in 73% of individuals who had orthodontic treatment [8-9]. Furthermore, automated image analysis of root canal and crown morphology and position can be applied to root canal treatment,

regenerative endodontic therapies, restorative crown shape planning to avoid inadequate forces on roots and planning of orthodontic tooth movement.

In this paper, automated root canal and crown segmentation algorithms as well as merging outputs of the different imaging modalities are proposed. The proposed patient specific classification and prediction tools are based on open-source software for both image processing and machine learning. The first tool is based on U-Net and Dumont et al.'s approach [10]; however, we did not use the same approach as we used upper jaw segmentations as well. RootCanalSeg tool is used for root canal automatic segmentation from cone-beam computed tomography (CBCT) images. We employ ResNet architecture in DentalModelSeg for automatic segmentation of digital dental models (DDM) acquired with intraoral scanners. The proposed method has three main stages which are (1) features extraction from raw volumetric and surface meshes, (2) identifying representative anatomic regions and (3) classification of voxel and meshes vertices. The outputs from RootCanalSeg and DentalModelSeg are then merged and labeled with the universal numbers used by clinicians; the merged file, as well as each individual pair of root and tooth, are saved in a folder.

The rest of the paper is organized as follows. In the next section we describe the dataset and the proposed method. In “Experimental Results” section, we present the results of the evaluation of the proposed methods using some metrics. Finally, we conclude the paper with suggestions for future research.

## MATERIAL AND METHODS

This retrospective study was approved by the institutional review board (IRB). The aim of this study was secondary data analysis and none of the CBCT scans were taken specifically for this research. The dataset consisted of 80 mandibular digital dental models (DDM), 40 for the upper and 40 for the lower dental arches, and 80 corresponding CBCT scans of the jaws. All subjects were imaged with the two imaging modalities. The mandibular CBCT scans were obtained using the Veraviewepocs 3D R100 (J Morita Corp.) with the following acquisition protocol: FOV 100 × 80 mm; 0.16 mm<sup>3</sup> voxel size; 90 kVp; 3 to 5 mA; and 9.3 seconds. DDM of the

\*Grant supported by NIDCR DE024450

<sup>1</sup> R. Deleat-Besson, C. Le, N. Al Turkestani, S. Brosset, M. Dumont, L. Cevdanes J. Bianchi, A. Ruellas, M. Gurgel, C. Massaro, A. Aliaga-Del Castillo, M. Ioshida, M. Yatabe, E. Benavides, H. Rios, F. Soki and G. Neiva are with the School of Dentistry, University of Michigan, Ann Arbor, MI 48109, USA, rdeleatb@umich.edu

<sup>2</sup> J. C. Prieto is with the Psychiatry, University of North Carolina, Chapel Hill, NC, USA

<sup>3</sup> J.F. Aristizabal is with the University of Valle, Cali, Colombia

<sup>4</sup> M. A. Alvarez and Diego Rey are with Department of Orthodontics, University of Medellin, Medellin, Colombia

<sup>5</sup> K. Najarian, W. Zhang, J. Gryak and R. Soroushmehr are with the Department of Computational Medicine and Bioinformatics, University of Michigan, Ann Arbor, MI 48109, USA

<sup>6</sup> J. C. Fillion-Robin and B. Paniagua are with Kitware Incorporation, Chapel Hill, NC, USA

mandibular arch were acquired from intraoral scanning with the TRIOS 3D intraoral scanner (3 Shape; software version: TRIOS 1.3.4.5). The TRIOS intraoral scanner (IOS) utilizes “ultrafast optical sectioning” and confocal microscopy to generate 3D images from multiple 2-dimensional images with accuracy of  $6.9 \pm 0.9 \mu\text{m}$ . All scans were obtained according to the manufacturer's instructions, by 1 trained operator. Two open-source software packages, ITK-SNAP, version 3.8 [11] and Slicer, version 4.11 [12] were used to perform user interactive manual segmentation of the volumetric images and common spatial orientation of the mandibular dental arches to train a model. We used a validated protocol described by Ioshida *et al* [13] to register IOS and CBCT scans to each other. Here, we propose a Patient Specific Classification and Prediction tool (PSCP) that includes RootCanalSeg and DentalModelSeg algorithm to merge the output of these tools and different imaging modalities for a better visualization of the teeth and roots.

**Automatic root canal segmentation.** As the contrast of CBCT scans is low, we first enhance the quality of the images in the pre-processing stage. Then, we increase the ratio between pixels belonging to root canals and background pixels to deal with the class imbalance issue. To do so, slice cropping on the axial plane was performed that increases the ratio between the pixels which belong to the root canals and the background pixels. The algorithm selected all the slices in each 3D scan in the dataset, split them into 2D cross-sections, and every cross-section was resized to 512 x 512 pixels. After the pre-processing stage, around 170 cross-sectional images were acquired for each patient (for a total of 13,600 samples) that were used to train a deep learning model using U-Net architecture [14, 15] for segmenting root canals. This network was developed initially for biomedical image segmentation and then employed in other applications, such as building extraction from high-resolution remote sensing images [16]. The training was performed with batch size of 11, 50 epochs and a learning rate of  $1e-4$ . As the images might be over/under segmented and there could be outliers in the results, we performed post-processing as follows. A threshold was set to 500 to remove small components and a k-mean with 2 classes was done to remove the second molars on the sagittal axis. An 8-fold cross validation was performed in which each fold contains 8 scans. The folds were created in a subject-wise manner (all scans from the same subject are contained within a single fold) and the distribution of the upper and lower scans within the folds were balanced. Therefore, 8 models were trained and for each model, seven folds (56 scans) were used for training and one fold (8 scans) was used as the validation set, the 16 remaining scans were used as the test set (for a total of 80 CBCT scans). To evaluate the performance of the proposed method, quantitative measurements such as Area Under the Receiver Operating Character Curves (AUC), F1 Score, sensitivity, specificity, and accuracy were computed. Then, we selected the best trained model based on the AUC metric and used it as the reference model for the segmentation.

**Automatic dental crowns segmentation.** Extracting shape features of the dental crowns could help analyzing the 3D dental model surfaces. In this paper, we propose an approach that takes 2D images of the 3D dental surface and extracts their associated shape features and the corresponding labels (background, boundary between teeth and gum, gum, teeth). We employ a region growing algorithm to generate the ground truth labeling of the dental surface. In this approach the minimum curvature is used as a stopping criterion plus manually correcting the miss-classified regions. We center and scale the mesh inside a sphere of radius one to generate the 2D training samples. We employ an icosahedron subdivision approach to sample the surface of the sphere where each sample point is used to create a tangent plane to the sphere. The tangent plane serves as the starting point of a ray-cast algorithm, *i.e.*, the dental surface is probed from the tangent plane. We employ the surface normal and the distance to the intersection as imaging features if an intersection is found. The corresponding ground truth label map is also extracted using a method described in [10]. We use the image pairs to train a modified U-Net model with connections like a ResNet [17]. In the modified U-Net, referred to as Ru-Net [18], the up-sampling block is modified to mirror the down-sampling blocks of ResNet. As a single point on the dental surface may be captured by several tangent planes, we employ a majority voting scheme on a new dental model where the label with the greater number of votes is set as the final label for a specific point on the surface. To remove islands or unlabeled surface points a post processing step is applied to find the closest connected labeled region. The output of this step is a mesh with labels 0 as gingiva, 1 as boundary and 2 as dental crown. The boundary helps label each crown with a unique label. Finally, the boundary between these regions is eroded to obtain a mesh with unique labels for each crown. The final model [19] was fed with  $80 \times 252$  (scans x images) equals 10,080 samples. The DMS tool, as part of the pipelines for PSCP tool, has been deployed in an open web-system for Data Storage, Computation, and Integration (DSCI) [20], for execution of the automated tasks [21].

**Merging root canals and crown segmentation.** Once we get the root canal segmentation and the crown segmentation, we perform the labeling of the teeth with specific labels following the Universal Numbering System [22]. First, we train a custom classification algorithm using data augmentation to differentiate the output from DentalModelSeg between lower or upper jaws with an accuracy of 99% (see Table 1 below) we merge the root canals and the crown segmentation and then we align the model with the corresponding template that has the Universal Ids for each crown using the iterative closest point transform. We re-label them with the closest crown on the template.

**Table 1.** Metrics for the lower and upper jaw prediction model from the library scikit-learn

	Precision	Recall	F1-score	Dataset
Lower	0.99	1.00	0.99	200
Upper	1.00	0.98	0.99	200
Accuracy	NA	NA	0.99	400
Macro avg	0.99	0.99	0.99	400
Weighted avg	0.99	0.99	0.99	400

Then, we use a sphere where the output of DMS is inside, and we take 64 pictures of it through a spiral form approach which allows us to have a sequence of multiple point of view of the output. We extract the features of the sequence using the VGG19 model from Keras. The model is composed by 2 bidirectional LSTM layers (each of them has a unit of 64) and 1 dense layer (with a unit of 64). The training was done with 38 scans (80% of the dataset) which were randomly rotated 50 times each, a learning rate of  $1e-4$ , 5 epochs, a batch size of 32, a binary cross entropy loss and the “Adam” optimizer. The testing was realized with the 8 remaining scans (20% of the dataset).

## EXPERIMENTAL RESULTS

Here, we show the results of our proposed root canal and dental model segmentation using the images/surfaces shown in Figure 1:

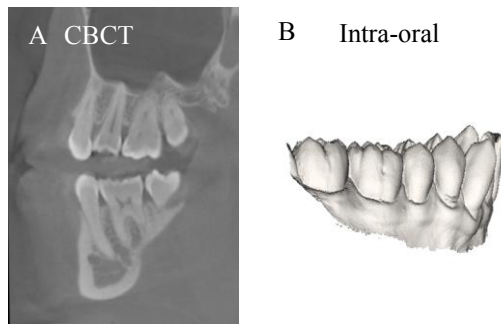


**Figure 1.** (A) A slice from a CBCT scan; (B) Dental model surface rendered on VTK.

**Automatic root canal segmentation.** The CBCT scans are put into slices and fed to the U-Net model to perform the root canal segmentation. Once the model segments the roots, we use a post-processing algorithm to remove artifacts from the segmentation. After the cleaning, we get the Figure 2. The result shown in Figure 2 is a representative of many cases from our dataset, which reveals that the automatic segmentation can identify the complete extension of the root canal until the root apex, compared to the manual segmentation. Therefore, the segmented pixels on the deeper parts of the root canals could result in increasing the number of false positives.

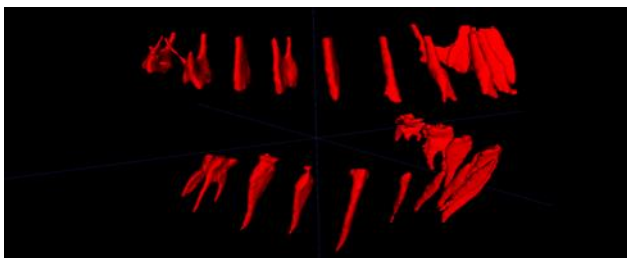


**Figure 2.** Upper and lower root canal segmentation

**Table 2.** Root canal segmentation metrics

Dataset	AUC	Sensitivity	Specificity	Accuracy	Mean F1
Validation std	0.95 $\pm 0.05$	0.87 $\pm 0.10$	0.99 $\pm 0.0001$	0.99 $\pm 0.0002$	0.73 $\pm 0.07$
Testing std	0.96 $\pm 0.04$	0.9 $\pm 0.09$	0.99 $\pm 0.0001$	0.99 $\pm 0.0002$	0.78 $\pm 0.07$

Table 2 shows that AUC, sensitivity, specificity, and accuracy are close to 1 which means that the model is performing well. On the other hand, the F1 score is a bit low and could be improved. However, the predicted segmentation is similar at 75% to the one done by clinicians and this low accuracy may be due to inconsistencies of the clinicians’ segmentation of the thin and tortuous root canals. A solution could be to use the prediction done by the model as the new segmentation. Then clinicians could correct them, and we would train a new model with the new segmented scans. Therefore, the F1 score metric should improve.

**Automatic dental crowns segmentation.** A continuous boundary between the crown and the gingiva is detected using the trained model which segments the individual dental crowns (Figure 3).

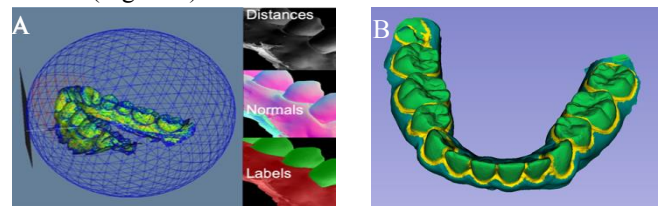


**Figure 3.** (A) The Icosahedron sphere to get the gingiva, gum and teeth label; (B) The dental model with the labels.

Once we get the dental model with the labels, we can easily separate the gum and the teeth, and label each one of them thanks to the DMS algorithm (Figure 4).

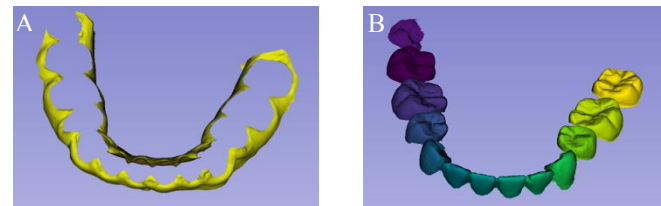


**Figure 4.** (A) The segmentation of the gum; (B) The teeth with a random label for each of them.

**Merging root canals and crown segmentation.** Once we get the teeth segmentation with their labels and the root canal segmentation, we merge them into a single surface for future quantitative assessments. There is also the possibility to acquire individual teeth segmentation for a better visualization (Figure 5).

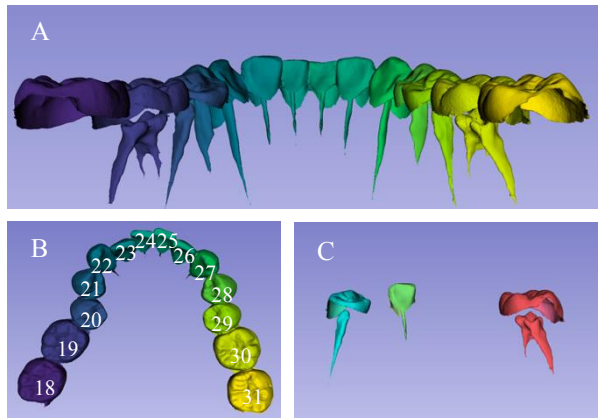


**Figure 5.** (A) Merging of root canal and teeth segmentation. In the original scan, there are only 14 teeth and 12 root canals segmented; (B) Labels of each tooth and root; (C) Three teeth that can be displayed individually.

## CONCLUSION AND FUTURE WORK

The chance of successful root canal preparation would increase and treatment of pulpally involved teeth would improve by root canal morphology identification. The root canal segmentation would also help indicate the root position for planning both orthodontic movements, restorative and/or implant dentistry. In this paper we proposed automated image processing and machine learning methods to segment both root canals and digital dental models automatically. The proposed methods could provide complementary information to the dental clinician by integrating the two imaging modalities. We first developed an automated root canal segmentation using CBCT images by training a U-Net model. We then employed a ResNet architecture for automatic segmentation of crowns using digital dental models. Those two methods have been merged to have a single 3D shape that possesses the Universal Ids used by clinicians on each tooth and root canal. F1 score values may still require further refinements because the data comes from one center and it may not generalize for other data. To make the model more generalizable and improve its performance, more samples for training the models will be added in our future work. Moreover, we will employ the trained models to segment new scans. The results could be used by clinicians to interactively modify them instead of manually segmenting the images from scratch. The training of the automatic dental crown segmentation algorithm was done with digital dental models of permanent full dentition. We used the trained model to segment dental crowns of the digital dental models in the primary and mixed stages of the dentition, in addition to cases with unerupted, missing or ectopically positioned teeth. The merging algorithm then integrates the two imaging modalities and allows clinicians to save each individual tooth and its root canal in separate folders. Such output files allow clinicians to plan treatment for specific teeth or regions of the dental arch rather than a single whole dental arch surface mesh. The

PSCP tools introduced in this paper are part of a clinical decision support system in dentistry that sheds light into gaps of knowledge, regarding tooth long axis for implant placement, restorative procedures, and biomechanics of tooth. The tools are deployed in the DSCI robust data management open web-system [20] that provides users with the spectrum of data science approaches from storage of collected data from different sources and image modalities to data processing and computation of data analytics. Future developments will allow automatic landmarks placement and quantitative approaches of tooth long axis.

## REFERENCES

- [1] Ko CC *et al.* Machine learning in orthodontics: application review. *Craniofacial Growth Series*, V. 56, 2020, pp 117-135, <http://hdl.handle.net/2027.42/153991>.
- [2] Xu X, *et al.* 3D tooth segmentation and labeling using deep convolutional neural networks. *IEEE trans vis comput graph.* 2019;25(7):2336-2348. doi: 10.1109/TVCG.2018.2839685
- [3] Elhaddaoui R *et al.* Resorption of maxillary incisors after orthodontic treatment-clinical study of risk factors. *Int Orthod* 2016; 14: 48-64. doi: 10.1016/j.ortho.2015.12.015
- [4] Marques LS *et al.* Severe root resorption in orthodontic patients treated with the edgewise method: prevalence and predictive factors. *Am J Orthod Dentofacial Orthop* 2010; 137: 384-8. Doi: 10.1016/j.ajodo.2008.04.024
- [5] Marques LS *et al.* Severe root resorption and orthodontic treatment: clinical implications after 25 years of follow-up. *Am J Orthod Dentofac Orthop* 2011; 139: S166-9. doi: 10.1016/j.ajodo.2009.05.032
- [6] Kamble RH *et al.* Stress distribution pattern in a root of maxillary central incisor having various root morphologies: a finite element study. *Angle Orthod* 2012; 82: 799-805. doi: 10.2319/083111-560.1
- [7] Oyama K *et al.* Effects of root morphology on stress distribution at the root apex. *Eur J Orthod* 2007; 29: 113-7. doi: 10.1093/ejo/cjl043.
- [8] Lupi JE *et al.* Prevalence and severity of apical root resorption and alveolar bone loss in orthodontically treated adults. *Am J Orthod Dentofacial Orthop.* 1996;109(1):28-37. doi:10.1016/s0889-5406(96)70160-9.
- [9] Ahlbrecht CA *et al.* Three-dimensional characterization of root morphology for maxillary incisors. *PLoS One.* 2017;12(6):e0178728. doi: 10.1371/journal.pone.0178728
- [10] Dumont M *et al.* Patient Specific Classification of Dental Root Canal and Crown Shape. *Shape Med Imaging* (2020). 2020 Oct;12474:145-153. doi: 10.1007/978-3-030-61056-2\_12.
- [11] ITK- snap, [www.itksnap.org](http://www.itksnap.org), accessed on November 01, 2020.
- [12] Slicer, version 4.11, [www.slicer.org](http://www.slicer.org), accessed on March 08, 2020.
- [13] Ioshida M *et al.* Accuracy and reliability of mandibular digital model registration with use of the mucogingival junction as the reference. *Oral Surg Oral Med Oral Pathol Oral Radiol.* 2019 Apr;127(4):351-360. doi: 10.1016/j.oooo.2018.10.003.
- [14] Ronneberger O *et al.* 2015, Oct. U-net: Convolutional networks for biomedical image segmentation. In international conference on medical image computing and computer-assisted intervention (pp. 234-241). Springer, Cham.
- [15] <https://github.com/zhixuhao/unet>, accessed on November 01, 2020.
- [16] Hosseinpoor, H. and Samadzadegan, F., 2020, February. Convolutional neural network for building extraction from high-resolution remote sensing images. In 2020 International Conference on Machine Vision and Image Processing (MVIP) (pp. 1-5). IEEE..
- [17] Ribera NT *et al.* Shape variation analyzer: a classifier for temporomandibular joint damaged by osteoarthritis. *Proc SPIE Int Soc Opt Eng.* 2019 Feb;10950:1095021. doi: 10.1117/12.2506018.
- [18] Alom, Md. Zahangir *et al.* (2018). Recurrent residual convolutional neural network based on U-Net (R2U-Net) for medical image segmentation. *arXiv:1802.06955*
- [19] DentalModelSeg source code and documentation, <https://github.com/DCBIA-OrthoLab/fly-by-cnn>, accessed on March 08, 2020.
- [20] Data storage computation and integration, DSCI, [www.dsci.dent.umich.edu](http://www.dsci.dent.umich.edu), accessed on March 08, 2020.
- [21] Michoud L *et al.* A web-based system for statistical shape analysis in temporomandibular joint osteoarthritis. *Proc SPIE Int Soc Opt Eng.* 2019 Feb; 10953:109530T. doi: 10.1117/12.250603.
- [22] Akshima Sahi (2019). Universal Numbering System for Teeth. <https://www.news-medical.net/health/Universal-Numbering-System-for-Teeth.aspx>
- [23] Michetti J *et al.* Comparison of an adaptive local thresholding method on CBCT and  $\mu$ CT endodontic images. *Phys Med Biol.* 2017; 63(1):015020. doi: 10.1088/1361-6560/aa90ff.